NIH Public Access
Author Manuscript
J Nanopart Res. Author manuscript; available in PMC 2013 December 01.

Published in final edited form as:
J Nanopart Res. 2012 December 1; 15: 1323–. doi:10.1007/s11051-012-1323-5.

A facile route to synthesize nanogels doped with silver nanoparticles

M. Carme Coll Ferrer[a,b], **Robert C. Ferrier Jr**[c], **David M. Eckmann**[b], and **Russell J. Composto**[*,a]

[a]Department of Materials Science, University of Pennsylvania, Philadelphia, US

[b]Department of Anesthesiology and Critical Care, University of Pennsylvania, Philadelphia, US

[c]Department of Chemical and Biomolecular Engineering, University of Pennsylvania, Philadelphia, US

Abstract

In this work, we describe a simple method to prepare hybrid nanogels consisting of a biocompatible core-shell polymer host containing silver nanoparticles. First, the nanogels (NG, ~160 nm) containing a lysozyme rich core and a dextran rich shell, are prepared via Maillard and heat-gelation reactions. Second, silver nanoparticles (Ag NPs, ~5nm) are synthesized *in situ* in the NG solution without requiring additional reducing agents. This approach leads to stable Ag NPs located in the NG. Furthermore, we demonstrate that the amount of Ag NPs in the NG can be tuned by varying silver precursor concentration. Hybrid nanogels with silver nanoparticles have potential in antimicrobial, optical and therapeutic applications.

Keywords

dextran; lysozyme; nanogel; silver nanoparticles

Introduction

The resistance of pathogenic bacteria to various antibiotics has promoted the study of silver nanoparticles (Ag NPs) as an antimicrobial agent because Ag NPs exhibit unique chemical and physical properties that are amplified at the nanoscale, i.e., high surface to volume ratio (Morones 2005, Rai 2009). Silver ions can disrupt biological processes. For instance, silver binds to thiols in bacterial membranes causing ion leakage and cell rupture and inactivates proteins responsible for RNA and DNA replication (Feng 2000, Lu 2008). Ag NPs can also induce an anti-inflammatory response as demonstrated with burn wound or peritoneal adhesion models (Wong 2010). These and other biological properties are the subject of intense research aimed at using Ag NPs in bio-applications in disease diagnosis, treatment and imaging. For instance, surface-enhanced Raman spectroscopy (SERS) was used to detect strains of the respiratory syncytial virus using substrates composed of silver nanorods (Shanmukh 2008) and more recently, Ag NPs (~ 20 nm) stabilized with egg white were used to enhance efficacy in radiotherapy using 231 tumor cells (Lu 2012). Reviews on therapeutic properties of Ag NPs such as antibacterial, antiviral, antifouling and targetting of cancer cells, are available in the literature (Nair 2007, Vaidyanathan 2009). Working with common materials, we have developed a novel and simple synthesis route for creating nanosized silver particles inside a relatively inert nanogel particle. The method presented makes readily

[*]Phone (215)-898-4451 Fax: (215)-573-2128 composto@seas.upenn.edu.

NIH-PA Author Manuscript
NIH-PA Author Manuscript
NIH-PA Author Manuscript

NIH-PA Author Manuscript

NIH-PA Author Manuscript

NIH-PA Author Manuscript

accessible an approach for controlled production of hybrid particles for delivery, imaging and other biomedical applications.

Studies suggest that Ag NPs can be non-toxic. However, cytotoxicity concerns have emerged due to the widespread use of NPs in medicine and other fields (Chen 2008). To increase the efficiency of silver nanoparticles while limiting their cell uptake and therefore possible cytotoxicity, we propose to deliver them inside a biocompatible nanogel (NG) consisting of a lysozyme core and dextran shell (Ferrer, Sobolewski 2012). Lysozyme is a positively charged enzyme (14.7 kDa) found in human tears, saliva, mucus and milk, which consists of a single polypeptide of 129 amino acids and 4 disulfide bonds and folds into a compact globular structure. Dextran, a neutral polysaccharide synthesized by bacteria, is used extensively in medical applications. The presence of dextran in the nanogel shell ensures stability over broad ranges of pH, ionic strength and temperature. More importantly, dextran imparts the NG with a “stealth-like” property that allows them to avoid mononuclear phagocyte system recognition. Additionally, dextran presents multiple hydroxyls that allow for attachment of ligands for specific biological applications. Hybrid NG reported in the literature include pH responsive poly(N-isopropylacrylamide) co-allylamine (PNIPAM-co-ALA) NG (James 2011), prepared with a Ag NP (36 nm) and thermo-responsive poly(N-isopropylacrylamide-co-acrylic acid) (PNIPAM-co-AA) NG (Wu 2010) with Ag NPs of undetermined size in the core prepared *in situ* using silver nitrate ($AgNO_3$). Note that both types of NG were composed of non-degradable, synthetic polymers and their preparation involved complex synthesis such as emulsion polymerization for the former and precipitation polymerization for the latter.

This communication describes the *in situ* synthesis of an ensemble of Ag NPs located in a NG made of lysozyme and dextran. Other than the $AgNO_3$ to synthesize the Ag NPs, this methodology does not require any other chemicals. Figure 1 is a schematic illustrating the three steps to synthesize NG with Ag NPs. The neat and hybrid NG are characterized by dynamic light scattering (DLS), ultraviolet-visible spectroscopy (UV-VIS), atomic force microscopy (AFM), thermogravimetric analysis (TGA) and transmission electron microscopy (TEM).

Experimental

The synthesis of NG was adapted from previous reported studies (Li 2008). Briefly, dextran from *Leuconostoc* ssp. and lysozyme were dissolved (1:1) in water, the pH was adjusted to 7-8 using 0.1 N sodium hydroxide, and the solution was lyophilized. The lyophilized powder was reacted at 60°C under 79% relative humidity in a desiccator containing saturated KBr solution for 24 hours. The reacted powder was dissolved in water (5 mg/mL), the pH was adjusted to 10.7 using 0.1 N sodium hydroxide, and the solution was further reacted at 80°C for 30 min. The resulting NG were purified by centrifugation using Amicon ultra 0.5 mL centrifugal filter devices with a 100 kDa molecular weight cut off (Millipore, Billerica, MA) and were stored in the dark at 4°C.

To prepare the hybrid NG, simply 2 mL of NG solution were mixed with 1 mL of $AgNO_3$ and autoclaved for 5 min using a Sterilimatic sterilizer (Market Forge Industries Inc., Everett, MA). The free Ag NPs were separated from the NG by dialysis in deionized water (49 mL), using a semi-permeable regenerated cellulose tubing (Mw cut off 15 kD) for 3 days.

The particle size and size distribution of the hydrated nanogels (0.2-0.4 mg/mL) were determined by dynamic light scattering using a Malvern Zetasize Nano series instrument (ZS90) equipped with a 22 mW He-Ne laser operating at a wavelength of 633 nm. UV

NIH-PA Author Manuscript

NIH-PA Author Manuscript

NIH-PA Author Manuscript

spectra of NG solution (0.2-0.4 mg/mL) were recorded on a Varian spectrophotometer (Cary 5000 UV-vis-NIR). Surface topography images were recorded using atomic force microscopy (AFM, Pico Plus, Agilent Technologies, Santa Clara, CA). The sample was prepared by placing a dilute drop of the nanogel solution onto a silicon wafer. Images were obtained using TOP MAC tapping mode with non-coated silicon levers with a force constant of 0.5-9.5 Nm^{-1} and a tip radius < 2nm (NanoAndMore). Images were analyzed using Gwyddion (Czech Metrology Institute). Nanogel morphology was imaged by transmission electronic microscopy (TEM) on a JEOL JEM 2010 at 80 kV. The samples were prepared by placing a dilute drop of the nanogel solution onto a holey carbon TEM grid (Structure Probe, Inc.). The excess of liquid was removed via capillary action using a paper filter at the bottom of the TEM grid. TEM micrographs were analyzed using ImageJ (NIH, Bethesda, MD). The amount of silver (wt.%) in the NG was determined by thermogravimetric analysis (TGA) using a Universal V4.1D TA Instruments (SDT Q600) with 2-4 mg samples under air atmosphere. The NG solutions were first dried and dispersed in a little ethanol. The solution was placed in tared platinum pan and heated to 80 °C at 10 °C/min. The sample was held at 80 °C for 2 h for complete removal of the ethanol and allowed to cool down to room temperature. Next, the samples were heated to 100 °C at 10 °C/min and held for 30 min to ensure complete removal of moisture. Then, the samples were heated to 675°C at 10 °C/min and held for 120 min to ensure complete removal of organic matter.

Results and Discussion

Synthesis of NG

The NG were prepared following a two-step heating process as illustrated in Figure 1 (Li 2008). First, conjugates were prepared via a Maillard heating reaction. During this step, amino groups from the lysozyme reacted with the terminal carbonyl groups of the dextran in the KBr saturated atmosphere to form lysozyme-dextran conjugates. Second, NG were prepared via a heat-gelation reaction at 80 °C. By heating the aqueous solution of conjugates at 80 °C at the isoelectric point of the protein, the lysozyme partially denatured, forming physically cross-linked nanogels (Li 2008). The neat NG consisted of a lysozyme rich core and a dextran rich shell.

Synthesis of hybrid NG

Ag NPs were synthesized "*in situ*" in the NG solution without additional reducing agents as represented by Figure 1 (far right). The reaction was carried out using $AgNO_3$ as a precursor agent in a NG solution that acted as both a reducing and a stabilizing agent. Reaction conditions involved autoclaving the NG solution to reduce Ag^+ to Ag^0. By autoclaving the solution, the NG became sterilized for subsequent biological studies (e.g., cell uptake). Four initial concentrations of $AgNO_3$, 2 mM (NG-Ag2), 5 mM (NG-Ag5), 10 mM (NG-Ag10) and 25 mM (NG-Ag25) were studied. The free Ag NPs were separated from the NG by dialysis in deionized water. The final product was NG particles (~160 nm) embedded with Ag NPs.

Biomolecules with carboxyl, hydroxyl and amines groups and polysaccharides have been previously used to reduce and stabilize Ag NPs (Sun 2005, Eby 2009). In previous work, we demonstrated that oxidized dextran, i.e., aldehyde and hydroxyl groups, could reduce silver cations and stabilize the resulting Ag NPs in aqueous solution (Ferrer, Hickok 2012). Another hydroxyl based polysaccharide, starch, has also been employed to reduce Ag NPs in solution (Vigneshwaran 2006). Using light activation, Eby et al.(Eby 2009) employed lysozyme to synthesize Ag NPs in methanol, which allowed for easy transfer into aqueous solution. The reduction of silver employing an amine was first described by Luo et al. (2005) using polyethylenimine. Similar to their system, Ag NPs are formed at neutral pH

NIH-PA Author Manuscript

NIH-PA Author Manuscript

NIH-PA Author Manuscript

where the lysozyme has an overall positive charge. Although the exact mechanism of Ag NP formation in the NG is unclear, these previous findings suggest that both lysozyme and dextran contributed to the *in situ* synthesis and stabilization of Ag NPs.

Characterization of Hybrid NG

As the Ag NPs nucleated, the color of the solution changed from transparent to yellow/brown (Figure 2A), depending on the initial concentration of $AgNO_3$. Figure 2A shows the UV-VIS spectra for the neat NG and the NG-Ag in solution, after dialysis to remove free Ag. Due to lysozyme adsorption, the neat NG showed a shoulder at 280 nm superimposed on a scattering background that decays towards low values near 650 nm. For NG-Ag2, the absorbance increased between 275 nm and 550 nm relative to the neat NG. This absorbance was observed to increase as the $AgNO_3$ concentration increased to 5 and 10 mM. For NG-Ag25, strong absorbance due to the surface plasmon resonance from Ag NPs was observed at 420 nm. Thus, we attributed the increase in absorption in the NG-Ag2, NG-Ag5 and NG-Ag10 to the Ag NPs; however, because of the scattering from the NG and the low concentration of Ag, no adsorption peak was observed. The hydrodynamic diameter and size distribution of NG and NG-Ag2 are given in Figure 2B. All NG displayed a Gaussian size distribution at the $AgNO_3$ concentrations studied. A summary of the hydrodynamic ratio and full width at half maximum (FWHM) for the NGs is included in Table 1. The NG were stable in solution for several weeks (i.e., do not aggregate). For neat NG, the hydrodynamic diameter and FWHM were 164 ± 33 nm and 110 nm, respectively. For NG-Ag2, a slightly larger distribution was measured (FWHM = 140 nm), while maintaining a similar diameter (164 nm), indicating that incorporation of Ag did not significantly swell the NG. Similar dimensions were observed for NG-Ag5 and NG-Ag10 as shown in Table 1. We attributed this observation to the high water content inside the NG. Tapping mode AFM was used to image the morphology of the nanogel dried under room conditions. Figure 2C shows a 3D image of NG-Ag2 indicating a diameter of ~ 270 nm and height of ~ 60 nm. Upon drying the NG acquired an ellipsoidal shape with a smooth and featureless surface, indicating that the Ag NPs were embedded in the NG. Figure 3A-F shows representative TEM images for neat NG (Figure 3A-C) and NG-Ag2 (Figure 3D-F) under high vacuum conditions. Similar images were obtained for NG-Ag5, NG-Ag10 and NG-Ag25 (Figure S1A-I). A majority of the NG appeared as individual particles with a round shape (Figure 3A-D). The Ag NPs were observed within the NG, indicating successful removal of free Ag NPs by dialysis at 2, 5 and 10mM concentration of $AgNO_3$. Few free Ag NPs remained in NG-Ag25 indicating that further optimization of the purification process is required at high concentration of $AgNO_3$. At higher magnifications (Figure 3B-C and 3E-F) the size of the NG as well as the individual Ag NPs embedded inside of the NG were determined and are included in Table 1. Histograms of the size distributions for the NG (neat and NG-Ag2) and Ag NPs in the NG-Ag2 are shown in Figure 3G-I. For the neat NG, the average particle size and FWHM were 83 ± 13 nm and 38 nm, respectively, similar to the diameter and FWHM of NG-Ag2, 90 ± 19 nm and 38 nm, respectively. These diameters were smaller than that by AFM, probably due to a combination of tip deconvolution issues in AFM (i.e., overestimates the size) and different atmosphere conditions used to image the samples (i.e., room conditions for AFM vs high vacuum for TEM). The diameter of the Ag NPs inside the NG was 4.9 ± 1.6 nm (FWHM = 2.4 nm) with an average of 120 NPs per NG. The average particle size distributions for NG-Ag25 were similar to the above values but with a slightly larger distribution (FWHM=3 nm) although the average number of NPs per NG was greater, 234 (Figure S1E-F). Thus, upon increasing the Ag from 2 to 25 mM, the loading of Ag NPs increased by 2x. Using the radii from DLS and TEM to estimate the swollen and dried size, the volume of the swollen NG was about 6x greater than the sample dried under room conditions. This result indicated high water content inside the NG. Other concentrations studied, 5 and 10 mM, resulted in similar average particle size distribution as NG-Ag2.

NIH-PA Author Manuscript

NIH-PA Author Manuscript

NIH-PA Author Manuscript

The amount of silver (weight %) in the hybrid NG was measured by TGA (Table 1). Figure 4 shows the weight loss for pure dextran, pure lysozyme, neat NG, NG-Ag2 and NG-Ag25. Samples were held isothermally at 100 °C for 30 min to remove traces of water. With increasing temperature, pure dextran exhibited an onset of thermal degradation at about 285 °C, whereas pure lysozyme began to degrade near 245 °C. Compared at T ~ 335 °C, dextran had lost about 70 wt.% due to degradation of the glycoside ring, relative to only 35 wt.% loss for lysozyme. Dextran had completely degraded by 525 °C, whereas lysozyme remained up to 650 °C. As expected, the NG reflected the behavior of both components. For NG and NG-Ag2, the onset of thermal degradation was observed at ~ 260 °C and ~ 180 °C, respectively, slightly lower than pure dextran, followed by a 50 wt.% decrease in weight loss. A second phase of weight loss began at about 475 °C reflecting the degradation of lysozyme. However, the weight loss was less for the neat NG, which required annealing up to 625 °C before complete degradation was observed. The weight loss for NG-Ag25 showed similar behavior as NG-Ag2, although complete degradation occured at a lower temperature (about 40 °C lower than NG-Ag2), indicating that NG-Ag25 degraded more readily than NG-Ag2. These results were in agreement with the well-known property of silver metal to catalyze oxidative degradation of polymers (Hucknall 1974, Southward 2001). The residual weights relative to the dried samples (T = 100 °C) have been summarized in Table 1. The residual silver was 4.8 wt.% and 8.5 wt.% for NG-Ag2 and NG-Ag25, respectively. The low wt.% measured for NG-Ag25 compared to NG-Ag2 indicated that the additional Ag NPs were formed in solution and removed by dialysis during the purifying step. This assumption was confirmed by TGA (Figure S2). Prior to dialysis the residual weights relative to the dried samples were 6.1 and 20.4 wt.% for NG-Ag2 and NG-Ag25, respectively. Assuming diameters of 5 nm for Ag NPs and 90 nm for NG, the number of Ag NPs per NG were 280 and 496 for NG-Ag2 and NG-Ag25, respectively. These values were about twice as high as the number of particles estimated from TEM images possibly because TEM underestimated the number of Ag NPs due to overlapping of NPs. However, in both TEM and TGA studies the loading of Ag was about 2x greater for the NG-Ag25 system. Other systems studied, NG-Ag5 and NG-Ag10, showed Ag loading prior dyalisis of 6.1 and 7.7 wt.%, respectively. Following dialysis the loading of Ag reduced to 5.1 and 5.7 wt.% for NG-Ag5 and NG-Ag10, respectively. By comparing *in situ* synthesis of Ag NPs inside the NG at the different concentrations of $AgNO_3$ studied, NG-Ag2 results in the highest effective system with 78% of the Ag NPs located in the NG. With increasing $AgNO_3$ concentration, efficiency decreases to 68%, 44% and 42% for NG-Ag5, NG-Ag10 and NG-Ag25, respectively.

Conclusion

To summarize, we have presented an approach to incorporate Ag NPs into dextran-lysozyme NG. We have demonstrated that the amount of Ag in the NG can be controlled by varying the concentration of silver nitrate. The NG and Ag NP diameters are relatively constant corresponding to ~ 160 nm and 5 nm, respectively. This facile approach has great potential to formulate Ag NP doped NGs for use in medicine and other fields. Using simple modifications, these hybrid NG can be further functionalized with ligand moieties to target specific receptor molecules or with dextranase enzyme to facilitate controlled degradation.

Supplementary Material

Refer to Web version on PubMed Central for supplementary material.

NIH-PA Author Manuscript

NIH-PA Author Manuscript

NIH-PA Author Manuscript

Acknowledgments

We acknowledge the support of NIH Grants R01 HL060230 and T32 HL007954 and NSF Grants DMR09-07493 and DMR11-20901. The authors thank Matthew A. Caporizzo for assistance in AFM and Dr. A. R. McGhie for helpful discussions.

References

Chen X, Schluesener HJ. Nanosilver: A nanoproduct in medical application. Toxicology Letters. 2008; 176(1):1–12. [PubMed: 18022772]

Eby DM, Luckarift HR, Johnson GR. Hybrid Antimicrobial Enzyme and Silver Nanoparticle Coatings for Medical Instruments. Acs Applied Materials & Interfaces. 2009; 1(7):1553–1560. [PubMed: 20355960]

Feng QL, Wu J, Chen GQ, Cui FZ, Kim TN, Kim JO. A mechanistic study of the antibacterial effect of silver ions on Escherichia coli and Staphylococcus aureus. Journal of Biomedical Materials Research. 2000; 52(4):662–668. [PubMed: 11033548]

Ferrer MCC, Hickok NJ, Eckmann DM, Composto RJ. Antibacterial biomimetic hybrid films. Soft Matter. 2012; 8(8):2423–2431.

Ferrer MCC, Sobolewski P, Eckmann DM, Composto RJ. Cellular uptake and intracellular cargo release from dextran based nanogel drug carriers. Journal of Nanotechnology in Engineering and Medicine. 2012 (submitted).

Hucknall, DJ. Selective Oxidation of Hydrocarbons. Academic Press, Inc.; London: 1974.

James C, Johnson AL, Jenkins ATA. Antimicrobial surface grafted thermally responsive PNIPAM-co-ALA nano-gels. Chemical Communications. 2011; 47(48):12777–12779. [PubMed: 22046590]

Li J, Yu SY, Yao P, Jiang M. Lysozyme-dextran core-shell nanogels prepared via a green process. Langmuir. 2008; 24(7):3486–3492. [PubMed: 18302424]

Lu L, Sun RW-Y, Chen R, Hui C-K, Ho C-M, Luk JM, Lau GKK, Che C-M. Silver nanoparticles inhibit hepatitis B virus replication. Antiviral Therapy. 2008; 13(2):253–262. [PubMed: 18505176]

Lu RQ, Yang DP, Cui DX, Wang ZY, Guo L. Egg white-mediated green synthesis of silver nanoparticles with excellent biocompatibility and enhanced radiation ef. International Journal of Nanomedicine. 2012; 7(1):2101–2107. [PubMed: 22619546]

Morones JR, Elechiguerra JL, Camacho A, Holt K, Kouri JB, Ramirez JT, Yacaman MJ. The bactericidal effect of silver nanoparticles. Nanotechnology. 2005; 16(10):2346–2353. [PubMed: 20818017]

Nair LS, Laurencin CT. Silver nanoparticles: Synthesis and therapeutic applications. Journal of Biomedical Nanotechnology. 2007; 3(4):301–316.

Rai M, Yadav A, Gade A. Silver nanoparticles as a new generation of antimicrobials. Biotechnology Advances. 2009; 27(1):76–83. [PubMed: 18854209]

Shanmukh S, Jones L, Zhao YP, Driskell JD, Tripp RA, Dluhy RA. Identification and classification of respiratory syncytial virus (RSV) strains by surface-enhanced Raman spectroscopy and multivariate statistical techniques. Analytical and Bioanalytical Chemistry. 2008; 390(6):1551–1555. [PubMed: 18236030]

Southward RE, Stoakley DM. Reflective and electrically conductive surface silvered polyimide films and coatings prepared via unusual single-stage self-metallization techniques. Progress in Organic Coatings. 2001; 41(1-3):99–119.

Sun XP, Luo YL. Preparation and size control of silver nanoparticles by a thermal method. Materials Letters. 2005; 59(29-30):3847–3850.

Vaidyanathan R, Kalishwaralal K, Gopalram S, Gurunathan S. Nanosilver-The burgeoning therapeutic molecule and its green synthesis (Retracted article. See vol. 28, pg. 940, 2010). Biotechnology Advances. 2009; 27(6):924–937. [PubMed: 19686832]

Vigneshwaran N, Nachane RP, Balasubramanya RH, Varadarajan PV. A novel one-pot ‘green’ synthesis of stable silver nanoparticles using soluble starch. Carbohydrate Research. 2006; 341(12):2012–2018. [PubMed: 16716274]

NIH-PA Author Manuscript

NIH-PA Author Manuscript

NIH-PA Author Manuscript

Wong KKY, Liu X. Silver nanoparticles-the real “silver bullet” in clinical medicine? Medchemcomm. 2010; 1(2):125–131.

Wu W, Zhou T, Berliner A, Banerjee P, Zhou S. Smart Core-Shell Hybrid Nanogels with Ag Nanoparticle Core for Cancer Cell Imaging and Gel Shell for pH-Regulated Drug Delivery. Chemistry of Materials. 2010; 22(6):1966–1976.

NIH-PA Author Manuscript
NIH-PA Author Manuscript
NIH-PA Author Manuscript

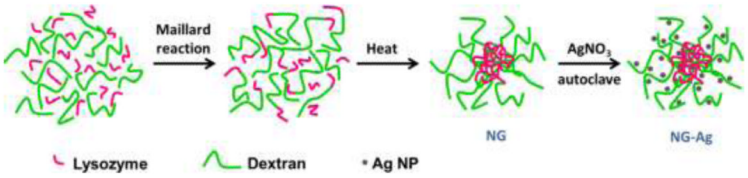

Figure 1.
Schematic drawing illustrating synthesis of neat NG and NG-Ag

NIH-PA Author Manuscript

NIH-PA Author Manuscript

NIH-PA Author Manuscript

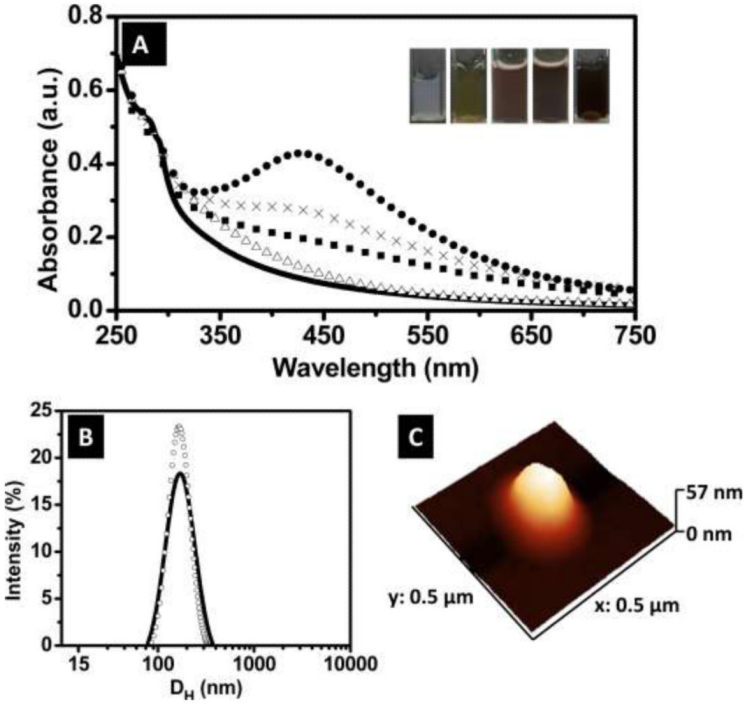

Figure 2.

(A) UV-VIS spectra for NG (line), NG-Ag2 (open triangles), NG-Ag5 (closed squares), NG-Ag10 (crosses) and NG-Ag25 (closed circles). The inset shows pictures of the hybrid NG (left to right): NG, NG-Ag2, NG-Ag5, NG-Ag10 and NG-Ag25 (B) Hydrodynamic diameter for NG (line), NG-Ag2 (open circles) and (C) AFM 3D topography image of NG-Ag2.

NIH-PA Author Manuscript
NIH-PA Author Manuscript
NIH-PA Author Manuscript

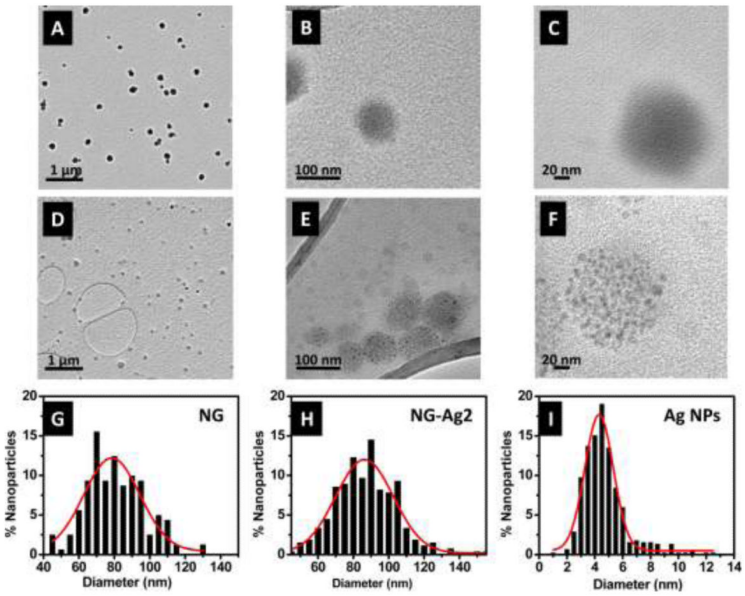

Figure 3.

TEM micrographs of (A-C) NG and (D-F) NG-Ag2. The histograms for particle size distribution are given in (G) NG, (H) NG-Ag2 and (I) Ag NPs in NG-Ag2. The red lines are Gaussian fits. The average particle sizes of NG and NG-Ag2 are 83 ± 13 nm and 90 ± 19 nm, respectively. The average size of Ag NPs is 4.9 ± 1.6 nm.

NIH-PA Author Manuscript

NIH-PA Author Manuscript

NIH-PA Author Manuscript

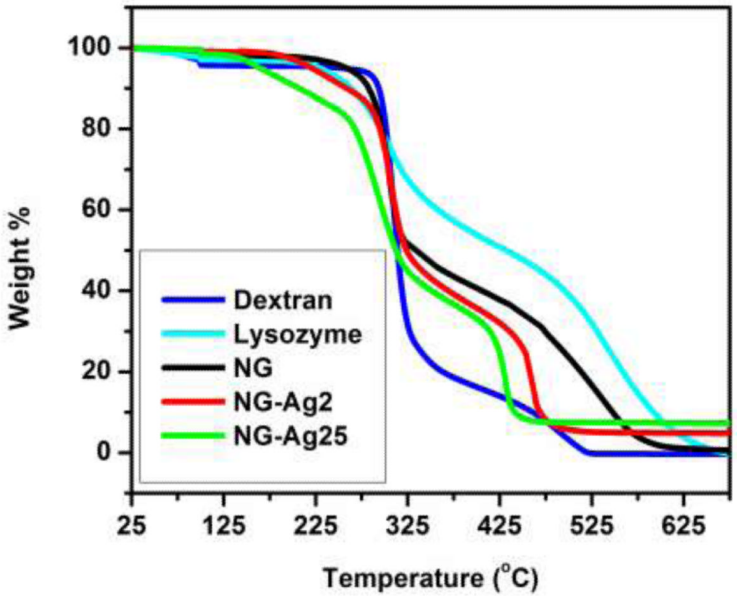

Figure 4.
TGA curves for dextran, lysozyme, neat NG, NG-Ag2 and NG-Ag25 in air. All samples were dried at 100 °C prior to heating.

NIH-PA Author Manuscript
NIH-PA Author Manuscript
NIH-PA Author Manuscript

J Nanopart Res. Author manuscript; available in PMC 2013 December 01.

Table 1

Summary of particle size distribution of NG as measured by DLS, NG and AgNPs in NG as measured by TEM and amount of Ag in the NG as measured by TGA.

Sample	Hydrodynamic diameter (nm) (DLS)		NG diameter (nm) (TEM)			AgNPs diameter (nm) (TEM)			Ag wt.%	
	D_H (nm)	FWHM	Mean ± sd	x_c	FWHM	Mean ± sd	x_c	FWHM	As prepared	After dialysis
NG	164 ± 33	110	83 ± 13	79	38	--	--	--	--	--
NG-Ag2	164 ± 43	140	90 ± 19	86	38	4.9 ± 1.6	4.3	2.4	6.1	4.8
NG-Ag5	177 ± 53	149	86 ± 16	80	30	4.2 ± 1.2	4.3	2.5	7.7	5.1
NG-Ag10	163 ± 41	120	86 ± 14	82	22	4.2 ± 1.1	4.4	2.2	12.9	5.7
NG-Ag25	168 ± 47	141	85 ± 20	80	31	4.6 ± 1.7	4	3	20.4	8.5

X_C: center of the Gaussian peak; FWHM: full width at half maximum of the Gaussian peak